

Atomic force microscopy investigations on nanoindentation impressions of some metals: effect of piling-up on hardness measurements

I. Jauberteau · M. Nadal · J. L. Jauberteau

Received: 22 February 2007 / Accepted: 8 July 2008 / Published online: 27 July 2008
© Springer Science+Business Media, LLC 2008

Abstract In the indentation test, the hardness and the elastic modulus depend strongly on the estimate of the indenter-material contact area at peak load. However, many elastic–plastic behaviours such as elastic recoveries during unloading and piling-up or sinking-in of surface profiles during indentation affect the determination of the hardness and the elastic modulus. So, atomic force microscopy is a method of utmost importance to provide an accurate knowledge of the indentation impression especially when plastic deformations occur, that leads to errors in the determination of the contact area. Atomic force measurements of vanadium, tungsten, molybdenum and tantalum pure metals as well as stainless steels, often used as substrates for thin films depositions, highlight the difficulties to estimate the contact area. The variation of hardness values determined by atomic force microscopy measurements and nanoindentation test is correlated to the formation of folds of 150 and 100 nm high, around the residual impression of vanadium and tungsten indented at 0.1 N, respectively. Some folds which increase with increasing loads are detected on the residual impressions of both 35CD4 and 30NCD16 stainless steels indented under loads of 0.01 N, only. Such structures are related to piling-up of surface profiles that could lead to an underestimate of the contact area in the indentation test. So, the hardness value of tungsten could be closer to 6 than to 7 GPa whereas the effect of piling-up on the estimation of contact

area of vanadium could be lower. Almost no deformation is seen on tantalum and molybdenum. So, the hardness values determined by the various methods are consistent. These results show that atomic force microscopy measurements are quite complementary of the nanoindentation test.

Introduction

Nanoindentation measurements at applied loads lower than 0.1 N provide mechanical data on the submicron scale of very thin films and surface layers without influence of substrates. Moreover they give local properties on nanocrystalline materials [1].

The indentation test consists of applying an increasing load on the surface of materials up to a maximum value then withdrawing fully the indenter. The sequence of loading and unloading may be repeated a few times to control the reversibility of the deformation and the recovering of elastic properties of materials during unloading (Fig. 1). In the elastic contact theory, the elastic modulus is derived from the following equation [2]:

$$S = \left(2/\pi^{1/2}\right)E_r(A)^{1/2}. \quad (1)$$

The stiffness S is mainly due to the elastic properties of the material and the indenter. Its value is experimentally measured from the slope of unloading at the maximum load. A is the projected area of elastic contact and E_r is the reduced elastic modulus, its value is given by the following equation:

$$1/E_r = (1 - \nu^2)/E + (1 - \nu_i^2)/E_i \quad (2)$$

where E , E_i , ν and ν_i are Young's modulus and Poisson's ratio for the material and the indenter, respectively.

I. Jauberteau (✉) · J. L. Jauberteau
UMR6638 CNRS, SPCTS, Faculté des Sciences
et des Techniques, Limoges cedex 87060, France
e-mail: isabelle.jauberteau@unilim.fr

M. Nadal
UPR8521 CNRS, LPMES, Tecnosud, Rambla de la
Thermodynamique, Perpignan 66100, France

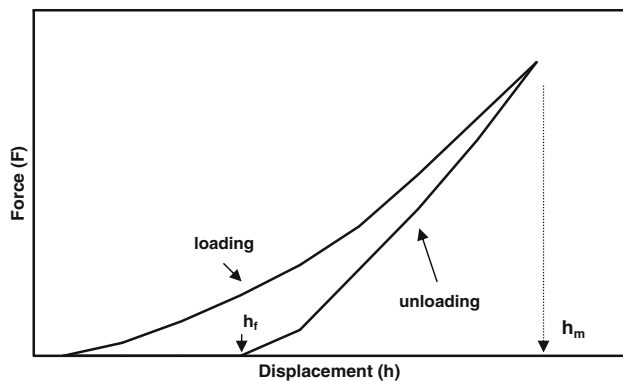


Fig. 1 A schematic representation of load versus indenter displacement, loading and unloading curves, h_f is the final depth and h_m the depth at peak load of the nanoindentation impression, respectively

The hardness is given by:

$$H = L_m/A \tag{3}$$

where L_m is the maximum indentation load.

Since A is the projected area of contact between the indenter and the material, its value is found from both the load–displacement data and the shape function of indenter. These calculations assumed that the material conforms to the shape of the indenter to some depth.

The method which consists of determining the diagonal length of indenter impression after the load is removed includes some errors which are mainly due to the varying elastic contraction of diagonal.

For a pyramid of ideal geometry (Berkovich indenter), the projected area of contact is given by:

$$A = 24.5 h_c^2 \tag{4}$$

where h_c is the depth of the indenter in contact with the sample under load. Since h_c is found after subtracting the elastic contribution of the maximum displacement of the indenter relative to the initial position of the surface, its value lies between the depth at peak load, i.e. the maximum displacement of the indenter and the residual depth of the indenter impression after unloading (Fig. 1). So, the main difficulty arises from the determination of the value of the depth of the indenter in contact with the sample and numerous recent papers are devoted to this parameter [3–5]. Because of the elastic recovery of the material under indenter unloading, the use of the residual depth instead of the contact depth leads to a significant overestimate of hardness.

By assuming that the material area in contact with the indenter remains constant during the first stages of unloading, Doerner and Nix [6] estimate the contact depth by drawing a straight line tangent to the unloading curve at the maximum load up to zero load. The depth of the indenter in contact with the material under load is then given by the intercept of the initial unloading slope with

the displacement axis. This method is successfully applied for flat punch indenter only. Since, the load–displacement relationships are not linear and the contact area changes continuously during unloading for indenters of geometries as solid of revolution, based on Sneddon’s solution of load, displacement and contact area relationship’s for indenter of solid, Oliver and Pharr [2] have introduced a relation between the deflection of the surface at the contact perimeter (indenter-material) and the indenter geometry ϵ

$$h_s = \epsilon L_m/S \tag{5}$$

where S is the stiffness as previously described, $\epsilon = 1, 0.75$ and 0.72 for flat punch, paraboloid of revolution and conical indenters, respectively.

The contact depth is then determined by the following relation:

$$h_c = h_m - h_s \tag{6}$$

where h_m is the maximum displacement.

However, the behaviour of the surface under the load of the indenter as sinking-in and piling-up effects causes errors in estimating the contact depth. More recently Yang-Tse Cheng and Che-Min Cheng show that the method of Oliver and Pharr may be used for highly elastic materials, only. The method underestimates the contact area for elastic–perfectly plastic solids [7]. So, Yang-Tse Cheng and Che-Min Cheng have introduced a work-hardening exponent equal to zero for elastic–perfectly plastic solids and equal to 0.1 and 0.5 for most metals.

Since the residual contact area of the indenter at the surface of the material depends strongly on the elastic plastic properties of the material, a main stage in the determination of such a parameter consists of finding the area function by imaging the indentation impression.

Atomic force microscopy must be successfully used for such measurements at submicron size.

The aim of this paper is to study the hardness of tantalum, vanadium, molybdenum and tungsten pure metals as well as 30NCD16 and 35CD4 stainless steels often used as substrates for thin film deposition. The atomic force microscopy allows investigating the shape of the indentation impression very accurately. Elastic effects such as the elastic recovering during unloading can be detected as well as viscous-plastic behaviour as sinking-in and piling-up effects.

These effects play a great role in the measurements of mechanical properties of soft material coatings on hard substrates [8].

Experimental set-up

Sets of three indentation impressions are made on the surface of tantalum, vanadium, tungsten, molybdenum,

35CD4 stainless steel of nominal composition: 0.35% of C, 1.05% of Cr, 0.16% of Mo, 0.81% of Mn, 0.28% of Si, 0.02% of P and 0.03% of S and 35NCD16 stainless steel of nominal composition: 0.35% of C, 3.5 % of Ni, 1.5 % of Cr, 0.4 % of Mo, 0.19% of Mn, 0.23% of Si, 0.21% of N, 0.06% of Cu, 0.09% of Al, 0.06% of P and 0.001% of S, all contents being expressed as a percentage of the total mass [9]. Loads of 0.01, 0.05 and 0.1 N are applied, respectively, with a Berkovich diamond indenter of pyramidal geometry with a triangular base. The angle between the perpendicular axis drawn from the top of the pyramid to the base centre and a side is equal to 65.27° .

Nanoindentation tests have been carried out with a Nanoindenter II of the Nano Instrument Society [10]. The indenter is first loaded and the load is held constant for a period of 10 s, then it is unloaded at 90% of the peak value at 50% of the loading rate of 1 m N s^{-1} . A hold for a period of 100 s is performed to account for a possible thermal drift. A new sequence of loaded and unloaded with an unloading of 100% of the peak value is then performed.

The impressions are detected by means of an optical microscope. Atomic force measurements are conducted with a digital instruments nanoscope II operating in a constant force mode [11]. The heights profile is obtained after each (x,y) scan of up to $130 \mu\text{m} \times 130 \mu\text{m}$, the maximum value of height is about $5 \mu\text{m}$.

Based on the data provided by atomic force microscopy measurements performed on residual contact areas, the projected area of contact between the indenter and the material is calculated both from the length of the sides and from the depth of the impression with the following expressions:

$$A = \left(3^{1/2}/4\right)l^2 \quad (7)$$

where l is the length of the side of the impression.

$$A = 24.5 h^2 \quad (8)$$

where h is the depth of the impression.

The hardness is calculated from Eqs. 3 and 7 or 8 by using the mean value resulting from the measurements of the length of the three sides in one hand and in other hand from the measurement of the depth from the three corners or from the middle of the three sides of the impression (Fig. 2). The accuracy of the method is determined for each case from the measurements performing on three indenter impressions. Based on numerous data, the confidence interval is calculated by taking the relative measurement errors determined with a confidence level equal to 99% considering the student statistic law for sample size lower than 30. This leads to values of hardness within the accuracy of about 10%.

The atomic force images are neither filtered nor processed to avoid additional errors of measurements.

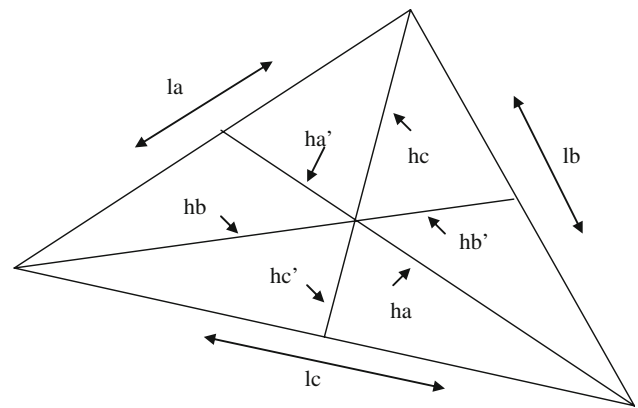


Fig. 2 A schematic representation of the residual nanoindentation impression, indicating the measurements of $l_{a,b,c}$ sides, $h_{a,b,c}$ depth from the corner and $h_{a',b',c'}$ depth from the middle of the sides of the residual indentation impression

However, since the surface is not quite horizontal, the values provided by each measurement are corrected by the value of the corresponding slope which is given by two points taken far from the indentation impression along the corresponding axis (Fig. 2).

The values of hardness are compared to those determined by the nanoindentation test. In that case, the hardness is calculated by using the semi-empirical method of Oliver and Pharr as previously introduced in the text. According to Eqs. 3, 4, 5 and 6 the hardness is obtained by measuring the following experimental data: L_m , h_m and S corresponding to the peak load, the depth at peak load and the initial unloading contact stiffness, respectively. S is found by analytically differentiating the following power law relation and evaluating the derivation at peak load and displacement.

$$L = A(h - h_f)^m \quad (9)$$

where the constants A , m and h_f (final depth) are determined by a least square fitting procedure.

Results and discussion

The values of the metals hardness found from the measurements of the length of the edges (H_l) and the depth of the residual impression (H_h) are indicated in Table 1. These values are compared with those obtained by means of the indentation test. Moreover, the influence of possible sinking-in or piling-up effects on the measurements of the hardness values is accounted by measuring the depth from the middle of the edges of the impression ($H_{h'}$).

As seen in Table 1, except for molybdenum indented under loads of 0.01 N, the values of hardness corresponding to pure metals indented under loads of 0.01 and 0.05 N

Table 1 Hardness values calculated from the measurements of the edge length (H_l), the depth from the corners (H_h), and the depth from the middle of the edges ($H_{h'}$) of the impressions and compared with the values obtained from the nanoindentation test (H_{nano})

Metal L (N), H (GPa)	W	V	Ta	Mo	35CD4 steel	30NCD16 steel
0.01, H_l	7.7	2.5	2.75	4.4	3.3	6.6
0.01, H_h	7.5	2.7	2.4	4.95	2.3	5.7
0.01, $H_{h'}$	7.5	2.7	2.4	3.6	1.8	4
0.01, H_{nano}	7.6	2.55	2.15	4.15	2.85	5.75
0.05, H_l	6.4	2.2	2	3.6	2.6	5.9
0.05, H_h	6	3	1.9	4	2.4	4.8
0.05, $H_{h'}$	6	2.2	1.9	3.6	1.9	3.5
0.05, H_{nano}	7	2.2	1.7	3.35	2.65	5.25
0.1, H_l	6	2	2	3.4	2.6	5.7
0.1, H_h	6.4	2	1.4	3	2.4	5.4
0.1, $H_{h'}$	5.2	1.4	1.4	2.7	1.9	4
0.1, H_{nano}	6.95	2.1	1.6	3.3	2.5	5.1

are fairly similar within the accuracy previously described, whatever the method used for the calculation of hardness.

The values of hardness calculated from the length of the edges, from the depth measured from the corners or from the middle of the edges of the nanoindentation impression are especially in good agreement with the reported values arising from the nanoindentation test for tungsten and vanadium indented under loads of 0.01 N and for vanadium, tantalum and molybdenum indented under loads of 0.05 N.

Indentations made on tungsten and vanadium under loads equal to 0.1 N lead to a quite different results since the measurements of the depth from the middle of the edge of the impression results in a lower hardness. This value is strongly correlated to the shape of the impression since as indicated in Fig. 3, some folds of 100 and 150 nm high are clearly detected around the impressions of tungsten and vanadium indented under loads of 0.1 N, respectively.

The formation of folds around the indenter impression is correlated to piling-up of the surface profiles during indentation. So, the contact area indenter-material is higher than the contact area determined by the conventional indentation test. Because of the strong plastic behaviour of tungsten, the hardness values determined from the nano-indentation test could be slightly underestimated. As reported above, the Oliver and Pharr procedure is not accurate enough for such metals especially when piling-up of surface profiles occurs. So based on Table 1, the hardness value of tungsten could be closer to 6 than to 7 GPa. A few plastic zones have been already reported on tungsten [12]. Since hardness values of vanadium determined by atomic force measurements are more consistent with those determined by the indentation test than in the case of tungsten, the piling-up effect on the determination of the contact area is lower for vanadium. Such tungsten and vanadium behaviours could be correlated to the strong dissimilarity between their elastic modulus which are equal to about 132 and 412 GPa, respectively. In contrast to these previous results, the deformations are quite low on the residual impressions corresponding to tantalum and molybdenum indented under the same conditions (Fig. 4). So the values of the hardness measured from h and h' are quite similar, that results in a fair agreement between the values of hardness determined by the various methods.

The behaviours of 35CD4 and 30NCD16 stainless steels under the indenter are quite similar. As reported in Table 1, the values of hardness determined from the depth measured from the middle of the edges are the lowest even for loads of 0.01 N, only. As for pure metals, the hardness values calculated from the depth measured from the corners of the indentation impression are consistent with the values determined from the length of the edges and also from the nanoindentation test within the accuracy of the measurement. These results are well correlated with the shape of the corresponding residual impressions since edge deformations

Fig. 3 Nanoindentation impressions made on tungsten and vanadium under loads of 0.1 N, (a) and (b), respectively

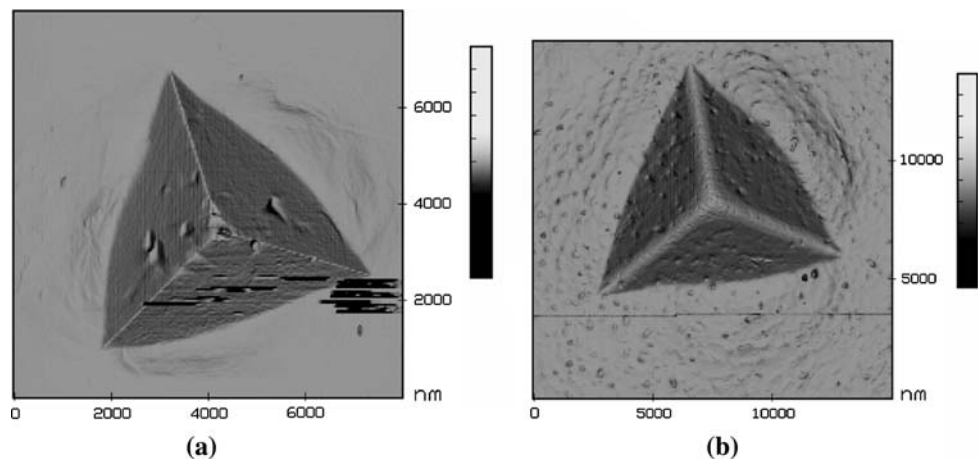


Fig. 4 Nanoindentation impressions made on tantalum and molybdenum under loads of 0.1 N, (a) and (b), respectively

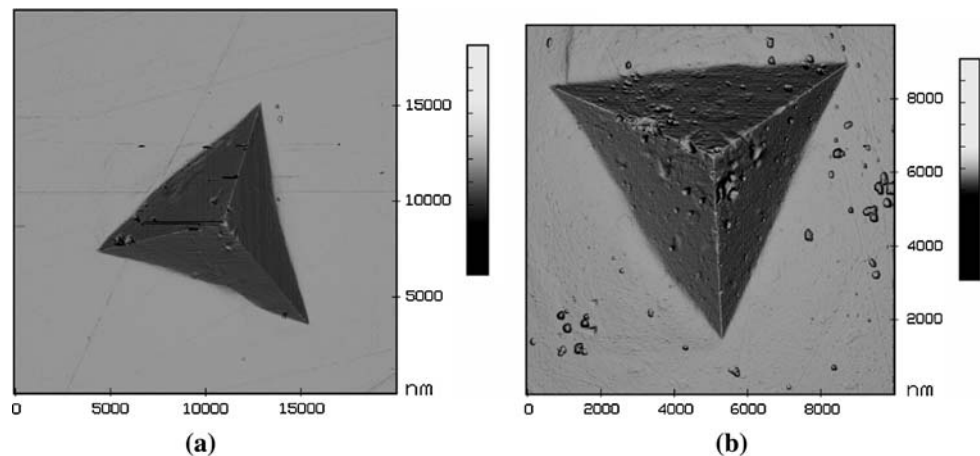
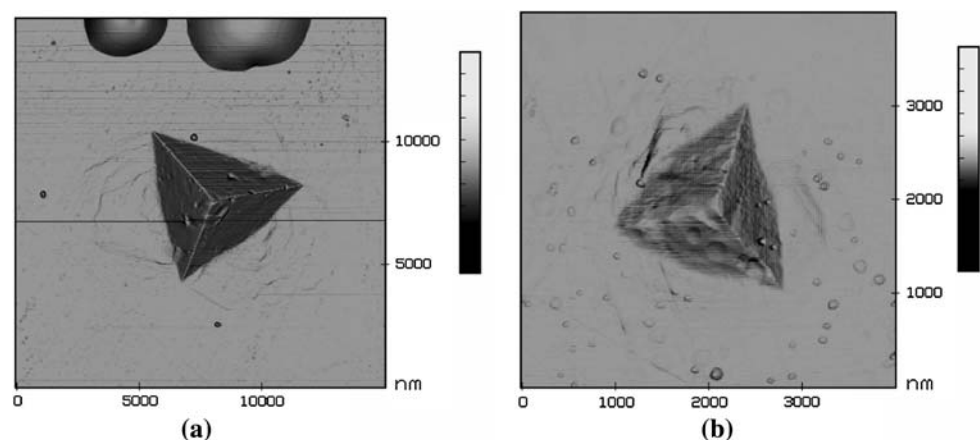


Fig. 5 Nanoindentation impressions made on 35CD4 steel under loads of 0.05 N and 30NCD16 steel under loads of 0.01 N, (a) and (b), respectively



are clearly seen around all the indentation impressions (Fig. 5).

The heights of such structures increases with increasing charge amount and are equal to 50, 100 and 150 nm at loads of 0.01, 0.05 and 0.1 N, respectively. All the results may be correlated to the elastic modulus of both steels which are similar and equal to about 215 and 230 GPa, respectively. These results show that the strong plastic behaviour of both stainless steels is correlated to piling-up of the surface profiles during the indentation, making the estimate of contact area difficult. So, the determination of hardness by the conventional indentation test should be used with caution.

Conclusions

Atomic force microscopy measurements allow imaging fruitfully the corresponding shape of nanoindentation impressions realized on pure metals or stainless steels at loads as low as 0.01 N. Because of the lack of accuracy in the estimate of the contact area between the indenter and the surface of plastic materials especially when piling-up

occurs, the conventional nanoindentation test should be used with caution. Some edges deformations are clearly seen around residual impressions corresponding to vanadium and tungsten indented under loads of 0.1 N. The tungsten hardness could be closer to 6 than to 7. Because of its large elastic modulus, the effect of piling-up on the estimate of the contact area indenter-vanadium could be lower and could not affect the hardness value. No deformations are detected around residual impressions of molybdenum and tantalum indented under similar conditions, so the hardness values of these metals determined with the various methods are quite consistent. For the both 35CD4 and 30NCD16 steels, the strong plastic behaviour under loads as low as 0.01 N make the estimate of the contact area more difficult. So, atomic force microscopy procedure is quite complementary of the conventional nanoindentation test.

References

1. Armstrong RW, Shin H, Ruff AW (1995) *Acta Metall Mater* 43:1037. doi:10.1016/0956-7151(94)00291-O

2. Oliver WC, Pharr GM (1992) *J Mater Res* 7:1564. doi:[10.1557/JMR.1992.1564](https://doi.org/10.1557/JMR.1992.1564)
3. Zhao ZX, Jiang ZD, Li XX, Gao ZK (2006) *Phys J Conference series* 48:1121
4. Fu G (2006) *Mater Lett* 60:3855. doi:[10.1016/j.matlet.2006.03.128](https://doi.org/10.1016/j.matlet.2006.03.128)
5. Troyon M, Liye H (2006) *Surf Coat Tech* 201:1613. doi:[10.1016/j.surfcoat.2006.02.033](https://doi.org/10.1016/j.surfcoat.2006.02.033)
6. Doerner MF, Nix WD (1986) *J Mater Res* 1:601. doi:[10.1557/JMR.1986.0601](https://doi.org/10.1557/JMR.1986.0601)
7. Yang-Tse C, Che-Min C (2000) *Surf Coat Tech* 133–134:417. doi:[10.1016/S0257-8972\(00\)00893-8](https://doi.org/10.1016/S0257-8972(00)00893-8)
8. Randall NX, Julia-Schmutz C, Soro JM (1998) *Surf Coat Tech* 108–109:489. doi:[10.1016/S0257-8972\(98\)00573-8](https://doi.org/10.1016/S0257-8972(98)00573-8)
9. Andrieux M, Ducarroir M, Ignat M, Mazot P, Angelelis C (1998) *Ann Chim Sci Mat* 23:847. doi:[10.1016/S0151-9107\(99\)80026-9](https://doi.org/10.1016/S0151-9107(99)80026-9)
10. Farges G, Sainte Catherine MC, Nadal M, Poirier L, Teyssandier F, Ignat M (1998) *Ann Chim Sci Mat* 23:863. doi:[10.1016/S0151-9107\(99\)80027-0](https://doi.org/10.1016/S0151-9107(99)80027-0)
11. Andrievski RA, Kalinnikov GV, Jauberteau I, Bates J (2000) *J Mater Sci* 35:2799. doi:[10.1023/A:1004790917616](https://doi.org/10.1023/A:1004790917616)
12. Kramer D, Huang H, Kriese M, Robach J, Nelson A, Wright A et al (1999) *Acta Mater* 47:333. doi:[10.1016/S1359-6454\(98\)00301-2](https://doi.org/10.1016/S1359-6454(98)00301-2)